

# Onset of a Bose-Glass of ultracold atoms in a disordered crystal of light

L. Fallani\*, J. E. Lye, V. Guarnera, C. Fort, and M. Inguscio

LENS European Laboratory for Nonlinear Spectroscopy and Dipartimento di Fisica, Università di Firenze  
via Nello Carrara 1, I-50019 Sesto Fiorentino (FI), Italy

Disorder is ubiquitous in nature, manifesting itself in many key physical and biological processes. It plays a fundamental role in the physics of conduction in metals and in the superfluid-insulator transition occurring in many condensed-matter systems. Ultracold atoms in optical potentials can be used as *quantum simulators* to model such disordered systems, taking advantage of the possibility to accurately control the kind and amount of disorder. Starting from a Mott Insulator state, we use a bichromatic optical lattice to add controlled disorder to an ideal optical crystal where bosonic atoms are pinned by repulsive interactions. Increasing disorder, we observe the onset of a gapless insulating Bose-Glass phase induced by the cooperation of interactions and disorder. This observation paves the way to the investigation of new strongly correlated disordered phases of broad interest even beyond the realm of physics.

## Introduction

Disorder is a key ingredient of the microscopic world. It plays a crucial role in statistical and condensed matter physics and it contributes in a substantial way to the mechanism of transport and conduction in ordinary crystals, where disorder is intrinsically present and cannot be controlled. As originally predicted by Anderson fifty years ago [1], disorder can lead to localization effects due to multiple interference of a wave scattered by random impurities. On the other hand, also interactions are well known to induce localization effects, as happens in the Mott Insulator (MI) phase [2, 3], in which a bosonic lattice system at zero temperature, instead of condensing in a superfluid (SF) state, forms an insulating “solid” state with integer filling of the lattice sites and vanishing phase coherence.

Much theoretical effort has been devoted to investigate the combined role of disorder and interactions in the superfluid-insulator transition observed in many condensed-matter systems, such as  $^4\text{He}$  adsorbed on porous media [4], thin superconducting films [5], arrays of Josephson junctions [6] and high-temperature superconductors [7]. If the disorder in the external potential is large enough, such systems are expected to enter an insulating state, the so-called *Bose-Glass* (BG), as predicted in a seminal paper by Fisher et al. [2], characterized by a gapless excitation spectrum and a finite compressibility. Despite the enormous interest in this phase and, more generally, in the phase diagram of disordered interacting quantum systems [8, 9, 10, 11], many fundamental problems are unsolved and still deserve investigation.

Ultracold atoms in optical lattices represent an extremely powerful tool for engineering simple quantum systems with a broad tunability of the Hamiltonian parameters, thus serving as “quantum simulators” [12] to reproduce the physics of different systems governed by the same laws. The striking advantage offered by such atomic systems resides in the unprecedented possibility to work with perfectly isolated samples at quasi-zero temperature and to have experimental access to many different parameters, such as the amount of interactions and

disorder, that can be precisely tuned even in real-time. One spectacular demonstration of this opportunity has been given by the observation of the SF to MI transition in a 3D optical lattice by Greiner et al. [3], which pioneered the investigation of strongly quantum correlated regimes with ultracold atoms [13, 14].

In this work we add controlled disorder to the crystalline structure exhibited by ultracold  $^{87}\text{Rb}$  atoms in the MI phase by using a non-commensurate periodic potential superimposed on the main lattice, that introduces a randomization of the energy landscape on the same length scale as the lattice spacing. As a result, the characteristic resonances in the energy spectrum of the MI state are lost and the system rearranges to form a state with a broadband excitability, where nonetheless superfluidity is inhibited by the varying site-to-site disorder, signaling the onset of a quantum phase transition to a new insulating BG phase.

## Adding disorder to an ideal crystal

At  $T = 0$  the many-body quantum state of an interacting gas of identical bosons in a lattice potential is well described by the Bose-Hubbard Hamiltonian [2]:

$$\hat{H} = -J \sum_{\langle j, j' \rangle} \hat{b}_j^\dagger \hat{b}_{j'} + \frac{U}{2} \sum_j \hat{n}_j (\hat{n}_j - 1) + \sum_j \epsilon_j \hat{n}_j \quad (1)$$

where  $\hat{b}_j$  ( $\hat{b}_j^\dagger$ ) is the annihilation (creation) operator of one particle in the  $j$ -th site,  $\hat{n}_j = \hat{b}_j^\dagger \hat{b}_j$  is the number operator, and  $\langle j, j' \rangle$  indicates the sum on nearest neighbors. Each of the three terms on the right-hand-side of Eq. (1) accounts for a different contribution to the total energy of the system:  $J$  is the *hopping energy*, proportional to the probability of quantum tunnelling of a boson between neighboring sites,  $U$  is the on-site *interaction energy*, arising from atom-atom on-site interactions (repulsive for  $^{87}\text{Rb}$ , for which  $U > 0$ ) and giving a nonzero contribution only if more than one particle occupies the same site, and  $\epsilon_j$  is a site-dependent energy accounting for inhomogeneous external potentials superimposed on

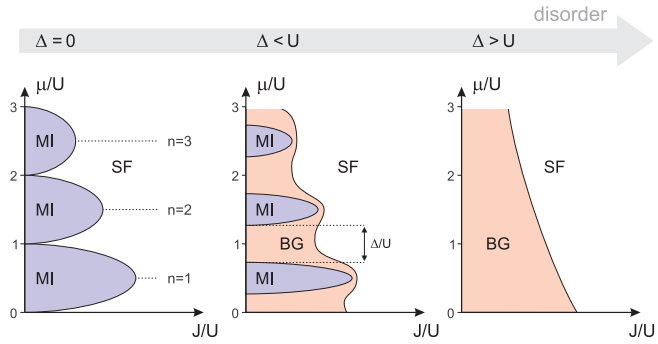


FIG. 1: Qualitative phase diagram for a system of interacting bosons as a function of the chemical potential  $\mu$  and of the three competing energy scales: tunnelling energy  $J$ , interaction energy  $U$  and disorder  $\Delta$ . Depending on the ratio between these quantities, the system rearranges to form a superfluid (SF), a Mott-Insulator (MI) or a Bose-Glass (BG) state.

the lattice. It has been suggested [15] and then experimentally demonstrated [3] that ultracold atoms in the lowest energy band of an optical lattice are indeed well modelled by this Hamiltonian. We note that Eq. (1) contains two main approximations: it takes into account only the lowest vibrational level of the lattice potential wells and considers only the coupling between nearest neighbors.

In the ideal case of a translationally invariant system, when  $\epsilon_j = 0$ , the ground state at  $T = 0$  is determined by the competition between the two energy scales  $J$  and  $U$  [3]. Assuming integer filling of the sites, when  $U \ll J$  the system is in a superfluid state, in which the bosons are delocalized across the lattice and the tunnelling ensures off-diagonal long-range coherence. Instead, when  $U \gg J$ , the system is in a localized *Mott insulator* state, where long-range phase coherence is lost and number Fock states are created at the lattice sites. The transition from a SF to a MI for ultracold atoms in a 3D optical lattice has been reported for the first time in [3], in which the ratio  $U/J$  was varied across the transition point by controlling the height of the lattice. The actual phase diagram of the system depends on the chemical potential  $\mu$  (related to the atomic density) and shows the existence of MI lobes with integer number of atoms per site, as qualitatively sketched in the left graph of Fig. 1

In the presence of a disordered external potential an additional energy scale  $\Delta$  enters the description of the system and is responsible for the existence of a new quantum phase at zero temperature. We consider the case of bounded disorder, in which  $\epsilon_j \in [-\Delta/2, \Delta/2]$ . In the presence of weak disorder  $\Delta < U$  the MI lobes in the phase diagram should progressively shrink and a new *Bose-Glass* phase should appear (central graph of Fig. 1), eventually washing away the MI region for  $\Delta > U$  (right graph of Fig. 1) [2]. This BG phase shares some properties with the MI state, namely both are insulating

states, with vanishing off-diagonal long-range coherence and vanishing superfluid fraction. However, differently from the MI, the BG should present a gapless excitation spectrum and a finite compressibility.

In order to better understand on a qualitative level the physics happening when approaching the BG phase, we consider the limiting case  $J \rightarrow 0$  and integer filling of the lattice sites. Naively speaking, in the MI phase one realizes a crystal of atoms pinned at the potential wells and sitting on the fundamental vibrational level, as schematically shown in Fig. 2. In a MI an energy gap in the excitation spectrum exists, since the elementary excitation - the hopping of a particle from a site to a neighboring one, or, in other words, the creation of a particle-hole pair - has an energy cost  $U$ , corresponding to the interaction energy of a pair of mutually repelling atoms sitting on the same site. In a BG, instead, one expects to observe a gapless excitation spectrum. The disappearance of the energy gap can be explained with a simple argument, considering that the presence of disorder introduces random energy differences  $\Delta_i \in [-\Delta, \Delta]$  between neighboring sites (see Fig. 2). As a consequence, the tunnelling of a boson through a potential barrier costs  $U + \Delta_i$ , that becomes a function of the position. The excitation energy is not the same for all the bosons, differently from the MI case, and one expects to observe a broadening of the resonance at energy  $U$ . In the full BG phase, when  $\Delta \gtrsim U$ , an infinite system can be excited at arbitrarily small energies and the energy gap shrinks to

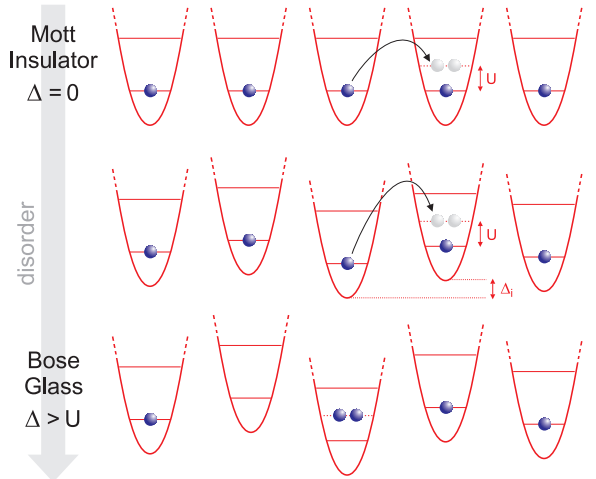


FIG. 2: In the Mott Insulator the tunnelling of one boson from a site to a neighboring one has an energy cost  $\Delta E = U$ , where  $U$  is the interaction energy of a pair of bosons sitting on the same site, and excitations at lower energies cannot be sustained. In the disordered case this excitation energy is  $\Delta E = U + \Delta_i$ , that becomes a function of the position, since the presence of disorder introduces random site-to-site energy differences  $\Delta_i$ . In the Bose-Glass state, in which  $\Delta_i > U$ , an infinite system could be excited at arbitrarily small energies and the energy gap would disappear.

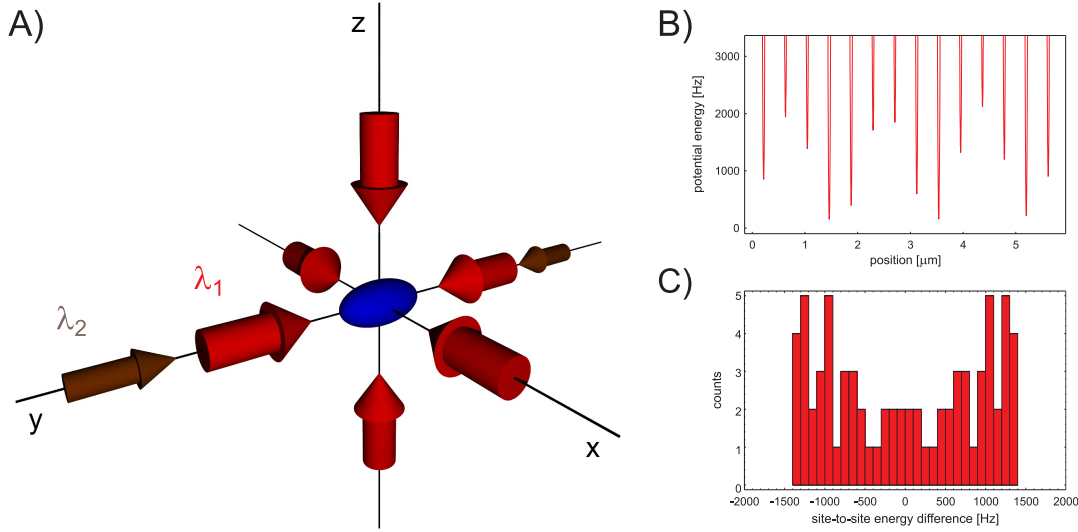


FIG. 3: A) An ultracold gas of  $^{87}\text{Rb}$  atoms (blue) is trapped in a deep 3D optical lattice with spacing  $\lambda_1/2$  created by three pairs of counterpropagating laser beams. An additional weak optical lattice with non-commensurate spacing  $\lambda_2/2$  (relatively to the main lattice) is superimposed along one of the main lattice directions. B) Scheme of the quasi-periodic potential energy resulting from the sum of the two lattices for a disordering lattice height  $s_2 = 1$  (corresponding to 1.98 kHz). C) Histogram of the energy differences between neighboring sites evaluated over an interval of  $\approx 70$  sites ( $30 \mu\text{m}$ ) for  $s_2 = 1$  and in the presence of the weak harmonic confinement present in the experiment [27].

zero. Despite the zero energy gap, excitations only occur locally between neighboring sites and the BG phase remains globally insulating.

### The disordered lattice

For a system of ultracold bosons in an optical lattice one can introduce controlled disorder in different ways. One possibility relies in laser speckles, i.e. laser light with a disorder intensity distribution produced by the reflection or transmission of a laser beam by a diffusing medium [16]. Experiments have already been realized with laser speckles in combination with atomic Bose-Einstein condensates with the aim to observe localization effects [17, 18, 19]. This technique, however, suffers a major limitation, that is the difficulty to create disorder on length scales smaller than several  $\mu\text{m}$ . In [17, 20] it has been shown that this disorder grain size is too large to observe quantum effects at the basis of Anderson-like localization of matter waves. In addition, the mean-field potential induced by atom-atom interactions can screen the disorder on a smaller length scale (healing length) than the disorder correlation length [19]. Different techniques have been recently proposed to overcome these limitations, exploiting the collisional interactions with randomly-distributed atoms of a different species [21] or the randomly-varying magnetic field in proximity of a current-carrying wire [22].

Optical disorder on a much smaller scale can be obtained by using two-color lattices [10, 11], i.e. superimposing on the already existing lattice with spacing  $d$  a second weaker lattice with different spacing  $d'$ . If the

two wavelengths are non-commensurate, one obtains a non-periodic deterministic modulation of the lattice potential at the beating frequency, thus breaking the discrete translational invariance of the lattice, analogously to what happens in optical quasi-crystals [23]. In the experiment, we use a Titanium:Sapphire laser operating at a wavelength  $\lambda_1 = 830 \text{ nm}$  to produce a three-dimensional optical lattice (*main lattice*). Disorder is then introduced by using an auxiliary lattice, obtained from a fiber-amplified diode laser emitting at  $\lambda_2 = 1076 \text{ nm}$  [24], aligned along one of the main lattice directions (*disordering lattice*), as schematically shown in Fig. 3A. The resulting potential can be expressed as

$$V(x, y, z) = s_1 E_{R1} (\sin^2 k_1 x + \sin^2 k_1 y + \sin^2 k_1 z) + s_2 E_{R2} \sin^2 k_2 y, \quad (2)$$

where  $s_1$  and  $s_2$  measure the height of the lattice potentials in units of the respective recoil energies  $E_{R1} = h^2/(2m\lambda_1^2) \simeq h \times 3.33 \text{ kHz}$  and  $E_{R2} = h^2/(2m\lambda_2^2) \simeq h \times 1.98 \text{ kHz}$ ,  $h$  is the Planck constant and  $m$  the mass of a  $^{87}\text{Rb}$  atom. When  $s_2 \ll s_1$  the disordering lattice has the only effect to scramble the energies at the bottom of the potential wells, introducing quasi-random energy costs for a particle to jump from a site to a neighboring one. The beating of the two laser standing waves along the common direction  $\hat{y}$  results in a non-periodic modulation of the main lattice potential with a length scale  $(2/\lambda_1 + 2/\lambda_2)^{-1} = 1.8 \mu\text{m}$ , corresponding to 4.3 lattice sites, as shown in Fig. 3B. The possibility to create non-periodic energy variations on the same length scale as the lattice spacing is a crucial improvement over speckles

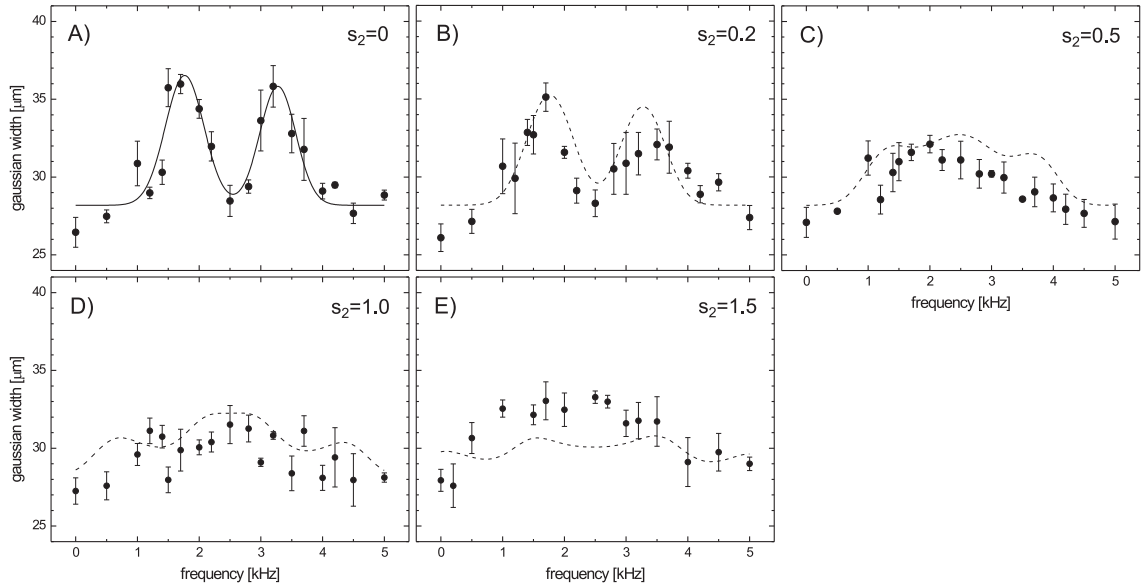


FIG. 4: Excitation spectra for a main lattice height  $s_1 = 25$  and different heights  $s_2$  of the disordered lattice. We report the width of the central peak in the time-of-flight density distribution after the excitation as a function of the modulation frequency. Points are averages of 3-5 different measurements, while error bars indicate the mean standard deviation.

experiments, in which the disordered potential typically varies on much larger distances, of the order of several tens of sites. In this bichromatic lattice the on-site energies can be calculated in the limit  $s_2 \ll s_1$  as

$$\epsilon_j = s_2 E_{R2} \sin^2\left(\frac{k_1 - k_2}{k_1} \pi j\right). \quad (3)$$

Even though this non-periodic modulation can be deterministically predicted, one expects that locally it can produce the same effects as the ones induced by a truly random potential, as suggested in recent theoretical works [10, 11]. In Fig. 3C we plot an histogram of the site-to-site energy differences occurring for  $s_2 = 1$  over a distance of  $30 \mu\text{m}$ , corresponding to the size of the atomic sample along direction  $\hat{y}$ , evidencing a quite flat distribution of energy differences.

We would like to stress that our realization of disorder produces just a weak modulation of the main lattice and has the only effect of randomizing the energies at the bottom of the sites. In particular, we can still consider the lattice to be composed of uniformly spaced potential barriers with the same height. When  $s_1 = 25$  and  $s_2 = 0.5$  the tunnelling energy  $J$  changes by less than 5% across the lattice, the interaction energy  $U$  changes by 1% and the distance between neighboring energy minima changes by 0.2%.

The disordered potential produced with this technique is stationary, with the phase of the two lattices staying constant on the timescale of the experiment. In particular, all the results presented below refer to a particular choice of the wavelengths and to a fixed realization of disorder. However, the degree of control on this system is

remarkable. The particular realization of disorder could be changed, even in real-time, by shifting the relative phase between the two lattices. In addition, by changing the wavelength of the disordered lattice (or changing the angle between the laser beams) it could be possible to change the spatial period of the modulation and, possibly, to evidence effects connected to the commensurability of the two periods [10].

## Experimental procedure and results

The source of ultracold atoms for the experiment is provided by a Bose-Einstein condensate of  $^{87}\text{Rb}$  produced by standard laser and evaporative cooling techniques. At the end of the cooling process we have a sample of  $10^5$  atoms confined in a magnetostatic trap at a temperature lower than 100 nK. In order to load the ground state of the lattice potential we adiabatically increase the intensity of the laser beams producing the 3D main lattice from zero to the final value, typically corresponding to  $s_1 = 25$ , using a 100 ms long exponential ramp with time constant 30 ms. After this loading procedure, we characterize the many-body state by measuring the excitation spectrum and observing the interference pattern after time-of-flight, i.e. switching off the confining potentials and imaging the density distribution of the atomic cloud after expansion.

The excitation spectrum is measured with the same Bragg spectroscopy technique adopted in [25], i.e. measuring the effect of an amplitude modulation of the lattice. In our experimental scheme a sinusoidal modulation with frequency  $\nu$  and amplitude 30% is applied to the

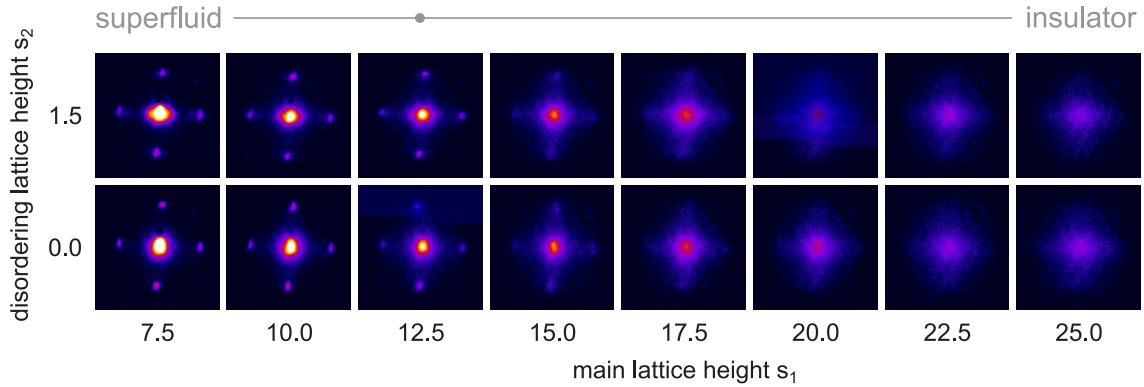


FIG. 5: Time-of-flight density distribution of the many-body ground state after release from the 3D lattice. The rows show the progression from a superfluid to an insulating state both in the absence of optical disorder  $s_2 = 0$  (bottom row) and for a height  $s_2 = 1.5$  of the disordering lattice (top row). Even if the excitation spectrum at  $s_2 = 1.5$  significantly differs from the  $s_2 = 0$  case, in the time-of-flight images we cannot detect any difference. The point marks the predicted lattice height for the transition from superfluid to Mott Insulator in an infinite homogeneous system with one atom per site. Each image is the average of 4 different images taken for the same parameters.

height of the  $\hat{y}$  direction of the main lattice [26]. This periodic variation of the lattice height stimulates the resonant production of particle-hole pairs with an energy  $h\nu$  set by the modulation frequency. We detect the excitations produced after 30 ms of modulation by first decreasing in 15 ms the intensity of the main lattice back to  $s_1 = 5$  in the superfluid phase, waiting 5 ms at this lattice height, then switching off all the confining potentials and imaging the atomic density distribution after time-of-flight. The width of the central peak in the density distribution is related to the energy transferred by the modulation to the atomic system, thus giving direct information on the possibility for the system to be excited at that particular frequency. A detailed description of this technique is contained in [25].

A typical energy spectrum for the MI state is reported in Fig. 4A, corresponding to  $s_1 = 25$  and  $s_2 = 0$ . Here it is possible to detect the presence of an excitation peak at frequency 1.7(1) kHz, close to the interaction energy  $U$  calculated at this lattice height. At almost twice the frequency 3.3(1) kHz it is possible to resolve a second peak [3], that can be attributed to higher-order processes and to excitations taking place at the boundary between different Mott domains. In the experiment the presence of a smooth harmonic confinement [27] is actually responsible for the existence of Mott regions with different number of atoms per site [28]. This weak confinement also contributes to the finite width of the resonances, that could be further increased by technical broadenings intrinsic in the excitation technique. We note that at  $s_1 = 25$  the tunnelling time is much larger than the duration of the modulation (at this lattice height the tunnelling energy is  $J \simeq 3.5$  Hz), hence excitations are mostly produced along the  $\hat{y}$  direction, where tunnelling is enhanced by the resonant reduction of the barriers height. This is also the direction along which the disordered potential is

applied.

Starting from this MI state, we can now add disorder to the main lattice in a controlled way by switching on the disordering lattice at different intensities. In the experiment, we adiabatically load the ground state of the bichromatic lattice by switching on both the lattices together using the same exponential ramp. Then we repeat the measurement of the excitation spectrum in the same way as described above. The results of such measurements are reported in Fig. 4B-E, for increasing disorder height from  $s_2 = 0.2$  to  $s_2 = 1.5$ . At a disorder height  $s_2 = 0.5$  (Fig. 4C), when the disordering lattice height is just 1% of the main lattice height, one already detects the disappearance of the characteristic peak structure of the MI and the appearance of a broader unstructured excitation spectrum. We note that at the largest disorder height  $s_2 = 1.5$  the maximum energy difference  $\Delta$  between neighboring sites corresponds to 2.0 kHz  $\simeq 1.1U$ , thus one expects to have already entered the full BG phase, with the complete disappearance of the MI state.

Additional information about the nature of the many-body ground state can be acquired by analyzing the time-of-flight images, that give an indication of the phase coherence of the system. In a SF state the atoms are delocalized and there is phase coherence across the lattice, resulting in well-resolved interference peaks. In an insulating state the atoms are pinned at the lattice sites and the lack of phase coherence results in a vanishing contrast in the interference pattern [3, 29]. In Fig. 5 we report false-color images of the atomic density distribution after a time-of-flight of 20 ms as a function of the main lattice height  $s_1$  both in the ordered case  $s_2 = 0$  and in the presence of the disordering lattice at  $s_2 = 1.5$ . In both the cases we observe the same progressive disappearance of the interference peaks when increasing the height of the main lattice. In particular, we would like to

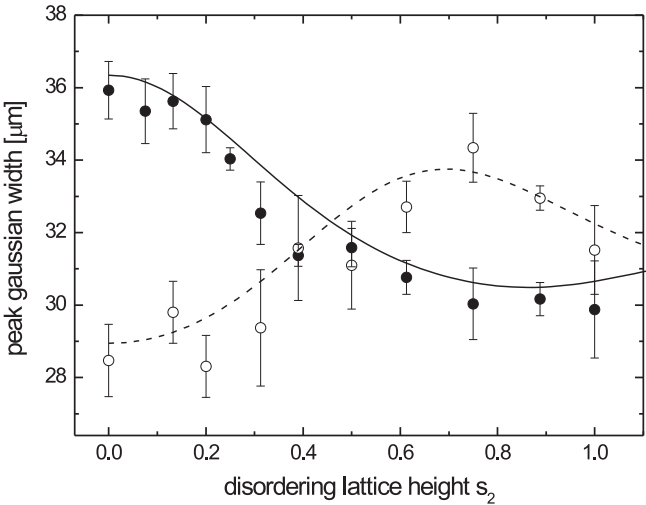


FIG. 6: Effect of the modulation at the MI excitation peak at 1.7 kHz (filled circles) and halfway between the MI peaks at 2.5 kHz (empty circles) for different heights of the disordering lattice from  $s_2 = 0$  to  $s_2 = 1$ . The lines are calculated from a model of inhomogeneous broadening of the MI resonances.

point out that for  $s_1 = 25$  and  $s_2 = 1.5$ , when the peaks in the excitation spectrum have already disappeared (see Fig. 4E), the time-of-flight picture clearly shows the existence of an insulating state.

The combination of the excitation spectra measurements and the time-of-flight images demonstrates that, with increasing disorder, the system goes from a MI state to an insulating state with an increasingly broader density of excitations, which can be identified with the BG state. Rigorously speaking, the BG phase should be characterized by a gapless excitation spectrum. Detecting the complete absence of a gap is technically impossible, since it would require a measurement of the possibility for the system to be excited at arbitrarily small energies (also where this modulation technique starts to be less efficient). In addition, the excitation spectrum is expected to be gapless only for an infinite system, while finite-sized systems always have discrete energy spectra. Nevertheless, we expect the density of excitations in a finite-sized BG to be significantly flatter than in the MI case [2]. In the following we will show that in the weak disorder regime the spectra in Fig. 4 can be explained with the inhomogeneous broadening of the MI peaks approaching the BG transition, accompanied by the consequent reduction of the energy gap, that is eventually washed away for strong disorder  $s_2 \gtrsim 1$ .

We have developed a simple model in which the MI resonances at  $U$  and  $2U$  are considered to be inhomogeneously broadened by the disordered distribution of site-to-site energy differences  $\Delta_i$ , that locally shift the position of the resonances. The broadened spectra are calculated by convolving the energy spectrum of the MI (fitted in Fig. 4A with a double gaussian, solid line)

with the actual distribution of energy shifts across the lattice [30]. The result of this convolution is reported in the dashed curves in Fig. 4B-E, showing a fine agreement with the experimental data for  $s_2 \leq 1$ . We find the agreement to be worse in the deep BG phase of Fig. 4E, in which  $\Delta > U$  and one expects a rearrangement of the atoms in a new insulating state with different site fillings, and the simple model of inhomogeneous broadening of the MI spectrum breaks down.

In order to more quantitatively analyze the progression from MI to BG, we report in Fig. 6 the width of the atomic density distribution after the excitation for a fixed modulation frequency of 1.7 kHz, corresponding to the first resonance peak in the MI excitation spectrum, and different disorder heights (filled circles). One clearly sees that the peak excitation starts to be suppressed even for very small disorder heights  $s_2 \lesssim 0.5$ , while the excitation at frequency 2.5 kHz, corresponding to the minimum between the MI peaks, starts to grow (empty circles), even exceeding the peak excitation for  $0.5 < s_2 < 1$ . In the same figure we also include the theoretical predictions based on the model described above (solid and dashed curves, for 1.7 kHz and 2.5 kHz respectively), showing that for  $s_2 < 1$  the experimental findings nicely match this picture of inhomogeneous broadening of the MI resonance. We note that the curves in Fig. 6 are not fitted to the experimental points, but result from a numerical calculation in which the only parameters extracted from the experiment are obtained from the gaussian fit of the spectrum at  $s_2 = 0$  shown in Fig. 4A. This mechanism has a spectroscopic analogy in the inhomogeneous broadening of spectral lines, occurring when each atom or molecule absorbs or emits at different frequencies (as happens in the case of crystalline solids due to the presence of defects). One expects the same kind of broadening to happen when approaching the transition from a MI to a BG phase, with the energy gap progressively closing with increasing disorder [9]. Eventually, when the broadening of the resonances reaches zero-energy and the gap completely disappears, the transition to a BG occurs, with a consequent rearrangement of the atoms in the lattice sites and a flat density of excitations deep in the BG phase [2]. The height of the resonance plotted in Fig. 6A (filled circles) could be used for the definition of a phenomenological order parameter, evidencing the building up of an ordered phase in the “low temperature” region (where the role of “temperature” is played here by the amount of disorder in the external potential).

## Outlook

Future advances of this work could be done in the direction of characterizing more in detail the phase diagram indicating the boundaries between the MI, SF and BG phases (qualitatively sketched in Fig. 1). In [2] it was argued that in the presence of weak disorder  $\Delta < U$  an intermediate BG state should exist between SF and MI even at integer filling. The exact nature of the phase

diagram, however, is still unclear, with some theoretical works providing numerical evidence for such an intermediate BG state [31] and other works presenting a different scenario [9, 32]. However, in the actual experiment the observation of such behavior could be complicated by the fact that an additional smooth harmonic confinement is present, introducing a continuous density-dependence that precludes the observation of pure bulk properties. The same kind of confinement also precludes a sharp phase transition between SF and MI. The transition point actually depends on the filling factor, that locally changes with the density, thus a mixed phase of SF and MI states is detected in proximity of the transition point, and is also responsible for the formation of Mott domains with different fillings deep in the MI phase.

Additional techniques could be implemented for a better diagnostic of the system, also in the “quantum simulation” perspective of using ultracold atoms to study these longly debated problems related to the exact nature of the phase diagram of disordered interacting systems. The standard way to distinguish a superfluid from an insulating phase consists in the time-of-flight analysis of the interference figure in the density distribution after release from the confining potentials, which gives information on the first-order (or phase) coherence of the many-body state. Additional information for the characterization of the BG state could be provided by novel interferometric techniques capable of detecting higher-order correlations, such as noise interferometry [33], that has been successfully applied to the study of spatial density correlations in the MI state [34] and to the detection of momentum correlations in paired fermions at the BEC-BCS crossover [35].

In principle, in order to further distinguish the BG from the MI state, one could measure the compressibility of the system, that could be accomplished by measuring the variation of volume of the sample after a change in the strength of the confining potential. Compressibility is expected to be finite in the case of BG and vanishing for a MI. However, the latter prediction is strictly valid only for a homogeneous system, or at least in the presence of just one Mott domain. In the presence of multiple Mott domains with different fillings, the system is locally incompressible, but globally compressible (since particles can be continuously redistributed among different Mott domains) [28].

Additional information for the characterization of the BG state could be obtained by investigating the dynamics of relaxation of the system after the production of

excitations, that should decay in time with the exponential behavior peculiar of glassy phases.

## Conclusions

In conclusion, we have reported on the first observation of the transition from a Mott Insulator, exhibiting insulating behavior and a gap in the excitation spectrum, to an insulating state with a flat density of excitations, that can be identified with the Bose-Glass phase. The progression between the two states is explored by adding controlled disorder on a system of ultracold atoms in a 3D optical lattice by means of an additional lattice with different spacing, that produces a quasi-randomization of the potential energies at the length scale of the single lattice site. This realization of disorder indeed represents a significant qualitative improvement with respect to previous experiments with ultracold atoms and is likely to allow the observation of other important disordered-related phenomena, such as Anderson localization, in a highly-controllable atomic system.

This work represents the opening of a new field of research, paving the way to the investigation of new strongly correlated quantum phases with ultracold atoms. Disorder can be introduced not only in the local chemical potential, as it has been done in this work, but also in other physical quantities, leading to different kinds of glassy phases. Among these, a magnetic system with random ferromagnetic/antiferromagnetic interactions is expected to form a spin glass [36]. Spin glasses deserve special attention because the theoretical formalism developed for their investigation can be used in different contexts, e.g. for modelling neural networks or different biological systems. In this perspective, ultracold Fermi-Bose mixtures in disordered potentials could be used to quantum-simulate a large variety of glassy phases, including spin glasses and quantum percolation systems [37]. Controlled disorder could also be used for quantum computation applications [38]. Disordered systems actually have a large number of local energy minima and could provide the possibility of storing quantum information by encoding it in robust metastable states.

From a more general point of view, we have demonstrated that ultracold atoms in a disordered potential can be used as a “nano-laboratories” in which it is possible to investigate fundamental disorder-related phenomena that infiltrate many different disciplines, from physics to life sciences, due to the underlying presence of disorder in nature.

---

[\*] Electronic address: [fallani@lens.unifi.it](mailto:fallani@lens.unifi.it)  
[1] P. W. Anderson, *Phys. Rev.* **109**, 1492 (1958).  
[2] M. P. A. Fisher, P. B. Weichman, G. Grinstein, and D. S. Fisher, *Phys. Rev. B* **40**, 546 (1989).  
[3] M. Greiner, O. Mandel, T. Esslinger, T. W. Hänsch, and I. Bloch, *Nature* **415**, 39 (2002).

[4] P. A. Crowell, F. W. Van Keuls, and J. D. Reppy, *Phys. Rev. Lett.* **75**, 1106 (1995); *Phys. Rev. B* **55**, 12620 (1997).  
[5] A. M. Goldman, and N. Marković, *Phys. Today* **51**, No. 11, 39 (1998).  
[6] H. S. J. van der Zant, F. C. Fritschy, W. J. Elion,

L. J. Geerligs, and J. E. Mooij, *Phys. Rev. B* **69**, 2971 (1992); H. S. J. van der Zant, W. J. Elion, L. J. Geerligs, and J. E. Mooij, *Phys. Rev. B* **54**, 10081 (1996).

[7] W. Jiang, N.-C. Yeh, D. S. Reed, U. Kriplani, D. A. Beam, M. Konczykowski, T. A. Tombrello, and F. Holtzberg, *Phys. Rev. Lett.* **72**, 550 (1994); R. C. Budhani, W. L. Holstein, and M. Suenaga, *Phys. Rev. Lett.* **72**, 566 (1994); T. Klein, C. Marcenat, S. Blanchard, J. Marcus, C. Bourbonnais, R. Brusetti, C. J. van der Beek, and M. Konczykowski, *Phys. Rev. Lett.* **92**, 037005 (2004).

[8] R. T. Scalettar, G. G. Batrouni, and G. T. Zimanyi, *Phys. Rev. Lett.* **66**, 3144 (1991).

[9] W. Krauth, N. Trivedi, and D. Ceperley, *Phys. Rev. Lett.* **67**, 2307 (1991).

[10] R. Roth and K. Burnett, *Phys. Rev. A* **68**, 023604 (2003).

[11] B. Damski, J. Zakrzewski, L. Santos, P. Zoller, and M. Lewenstein, *Phys. Rev. Lett.* **91**, 080403 (2003).

[12] R. P. Feynman, *Int. J. Theor. Phys.* **21**, 467 (1982); *Found. Phys.* **16**, 507 (1986); *Opt. News* **11**, 11 (1985).

[13] B. Paredes, A. Widera, V. Murg, O. Mandel, S. Fölling, J. Cirac, G. V. Shlyapnikov, T. W. Hänsch, and I. Bloch, *Nature* **429**, 277 (2004).

[14] T. Kinoshita, T. Wenger, and D. S. Weiss, *Science* **305**, 1125 (2004).

[15] D. Jaksch, C. Bruder, J. I. Cirac, C. W. Gardiner, and P. Zoller, *Phys. Rev. Lett.* **81**, 003108 (1998).

[16] J. E. Lye, L. Fallani, M. Modugno, D. S. Wiersma, C. Fort, and M. Inguscio, *Phys. Rev. Lett.* **95**, 070401 (2005).

[17] C. Fort, L. Fallani, V. Guarrera, J. E. Lye, M. Modugno, D. S. Wiersma, and M. Inguscio, *Phys. Rev. Lett.* **95**, 170410 (2005).

[18] D. Clément, A. F. Varón, M. Hugbart, J. A. Retter, P. Bouyer, L. Sanchez-Palencia, D. M. Gangardt, G. V. Shlyapnikov, and A. Aspect, *Phys. Rev. Lett.* **95**, 170409 (2005).

[19] T. Schulte, S. Drenkelforth, J. Kruse, W. Ertmer, J. Arlt, K. Sacha, J. Zakrzewski, and M. Lewenstein, *Phys. Rev. Lett.* **95**, 170411 (2005).

[20] M. Modugno, *Phys. Rev. A* **73**, 013606 (2006).

[21] U. Gavish and Y. Castin, *Phys. Rev. Lett.* **95**, 020401 (2005).

[22] H. Gimperlein, S. Wessel, J. Schmiedmayer, and L. Santos, *Phys. Rev. Lett.* **95**, 170401 (2005).

[23] L. Guidoni, C. Triché, P. Verkerk, and G. Grynberg, *Phys. Rev. Lett.* **79**, 3363 (1997).

[24] We acknowledge P. Cancio Pastor and P. De Natale from Istituto Nazionale di Ottica Applicata (INOA) for having provided this laser system.

[25] T. Stöferle, H. Moritz, C. Schori, M. Köhl, and T. Esslinger, *Phys. Rev. Lett.* **92**, 130403 (2004).

[26] We note that, when periodically lowering the lattice height during the modulation, the systems always remains in the MI phase.

[27] The harmonic confinement is provided both by the magnetic trap in which the sample is evaporatively cooled (which is present during the entire experiment) and by the optical force produced by the focused laser beams of the main lattice. The resulting trapping frequencies for  $s_1 = 25$  are  $\omega_x = \omega_z = 2\pi \times 100$  Hz and  $\omega_y = 2\pi \times 50$  Hz. The contribution of the disordering lattice to the harmonic confinement can be completely neglected.

[28] G. G. Batrouni, V. Rousseau, R. T. Scalettar, M. Rigol, M. Muramatsu, P. J. H. Denteneer, and M. Troyer, *Phys. Rev. Lett.* **89**, 117203 (2002).

[29] F. Gerbier, A. Widera, S. Fölling, O. Mandel, T. Gericke, and I. Bloch, *Phys. Rev. A* **72**, 053606 (2005).

[30] This analysis will be presented in larger detail in a forthcoming publication.

[31] N. Prokof'ev and B. Svistunov, *Phys. Rev. Lett.* **92**, 015703 (2004).

[32] J. Kisker and H. Rieger, *Phys. Rev. B* **55**, R11981 (1997).

[33] E. Altman, E. Demler, and M. D. Lukin, *Phys. Rev. A* **70**, 013603 (2004).

[34] S. Fölling, F. Gerbier, A. Widera, O. Mandel, T. Gericke, and I. Bloch, *Nature* **434**, 481 (2005).

[35] M. Greiner, C. A. Regal, J. T. Stewart, and D. S. Jin, *Phys. Rev. Lett.* **94**, 110401 (2005).

[36] M. Mezard, G. Parisi, and M. A. Virasoro, *Spin Glass Theory and Beyond* (World Scientific Publishing, 1987).

[37] A. Sanpera, A. Kantian, L. Sanchez-Palencia, J. Zakrzewski, and M. Lewenstein, *Phys. Rev. Lett.* **93**, 040401 (2004).

[38] V. Ahufinger, L. Sanchez-Palencia, A. Kantian, A. Sanpera, and M. Lewenstein, *Phys. Rev. A* **72**, 063616 (2005).

[39] This work has been funded by the EU Contracts No. HPRN-CT-2000-00125, MIUR FIRB 2001, MIUR PRIN 2005 and Ente Cassa di Risparmio di Firenze. We would like to acknowledge P. Zoller for critical reading of the manuscript. We also thank F. S. Cataliotti, M. Modugno, D. S. Wiersma and all the colleagues of the Cold Quantum Gases Group in Florence for useful comments, as well as R. Fazio and C. Tozzo from SNS for stimulating discussions.